RSC Advances

ROYAL SOCIETY OF CHEMISTRY

www.rsc.org/advances

RSC Advances

RSCPublishing

ARTICLE

Comparison of metal chloride-doped graphene electrode fabrication processes for GaN-based light emitting diodes

Cite this: DOI: 10.1039/x0xx00000x

Received 00th January 2012,
Accepted 00th January 2012

DOI: 10.1039/x0xx00000x

www.rsc.org/

Ki Chang Kwon,[a] Buem Jun Kim,[b] Cheolmin Kim,[a] Jong-Lam Lee,*[b] and Soo Young Kim*[a]

The effect of inductively coupled plasma (ICP) etching on the performance of light emitting diodes (LEDs) with doped graphene (D-G) electrodes was investigated. The sheet resistance decreased from 220 Ω/sq to 105–140 Ω/sq, and the value of the work function increased from 4.2 eV to the 4.9–5.1 eV range after four-layer graphene was doped with metal chlorides. The voltage at a 10 mA current was 5.5 V for LEDs with pristine graphene (P-G) and D-G electrodes when graphene was treated using the ICP etching step. The ICP etching process heated the D-G, recovering P-G properties in D-G and depositing residual photoresist on the graphene surface. Therefore, no difference was found in the electrical and luminance characteristics of P-G and D-G LEDs. The voltage at a 10 mA current was lowered to 4.25–4.5 V for LEDs using D-G electrodes without ICP etching. The luminance properties of these LEDS were improved compared to the LED with a P-G electrode. The decrease in the sheet resistance and increase in the value of the work function in D-G enhanced the electrical properties of the LEDs. Therefore, avoiding the ICP etching step is better for D-G electrodes in GaN-based LEDs.

Introduction

GaN-based light-emitting diodes (LEDs) with low operating voltage and high power have been rapidly developed for various applications, such as monitor displays, solid-state lighting, and traffic signals. Achieving high-quality and reliable ohmic contacts has been crucial for GaN-based LEDs since their development by Nakamura et al.[1] Various transparent conducting metal/metal oxide structures were used to obtain low-resistant and high-transparent ohmic contacts ($<10^{-4}$ Ω·cm^2, >90%) for p-type GaN. Among these contacts, oxidized Ni/Au and indium tin oxide (ITO) are widely used to form the current spreading layer. However, the amorphous Ni-Ga-O phase in the Ni/Au contact insulates the thin films at high current density.[2] In the case of ITO, the cost increase of indium, diffusion of indium to semiconductor phase, and low mechanical strength are still problems affecting high-power LEDs.[3] Therefore, research into excellent current spreading layer materials other than oxidized Ni/Au and ITO is needed to further develop LEDs with low operating voltage and high power.

Graphene has received much attention as an alternative electrode for *p*-type GaN because of its high carrier mobility (>200,000 cm^2·V^{-1}·s^{-1}), high transparency (>90%), and superior chemical resistance.[4-7] The forward voltage of LEDs with a multilayer graphene (MLG) electrode is reported to be 5.6 V at 20 mA because of the ambiguous work function and relatively high sheet resistance, which is equivalent to an ITO-based LED at 63% power output.[8] In order to reduce the sheet resistance of graphene and its contact resistance with p-type GaN, p-type GaN nanorods, $AuCl_3$-doped MLG, Ni/Au/$AuCl_3$-doped MLG, and Au/$AuCl_3$-doped MLG were investigated.[9-13] However, the operating voltage is still high because the fabrication process is not yet optimized. Therefore, a comparison of device properties according to the GaN LED fabrication process is needed to optimize these properties.

In this study, we compared two different LED fabrication methods that used inductively coupled plasma (ICP) etching, which is needed to open n-type GaN. Furthermore, the effect of multilayer doped graphene (D-G) on current spreading properties was investigated. D-G with metal chlorides using a layer-by-layer transfer method was used as the current spreading layer in p-type GaN-based LEDs. The changes in the work function value, G band in Raman spectra, and surface image after metal chloride doping on graphene and ICP treatment were analyzed using ultraviolet photoemission spectroscopy (UPS), Raman spectroscopy, and field-emission scanning electron microscopy (FE-SEM). From these data, the effect of metal chloride doped graphene and the LED fabrication process on LED performance was investigated.

Experimental Section

[a]*School of Chemical Engineering and Materials Science, Chung-Ang University, 221 Heukseok-dong, Dongjak-gu, Seoul 156-756, Republic of Korea. E-mail: sooyoungkim@cau.ac.kr*

[b]*Department of Materials Science and Engineering, Pohang University of Science and Technology (POSTECH), Pohang, Gyeongbuk 790-784, Republic of Korea. E-mail: jllee@postech.ac.kr*

Preparation of D-G graphene electrodes: Pristine graphene film (P-G) was grown using chemical vapor deposition on 25 μm copper foil with a methane and hydrogen gas mixture. After its growth, graphene was transferred to GaN substrates using polymethylmethacrylate (PMMA). After this transfer, the PMMA layer was removed using a boiled acetone bath at 50 °C. The metal chlorides were dissolved in coordinating solvents such as nitromethane, acetonitrile, and methanol for $AuCl_3$, $IrCl_3$, and $RhCl_3$. The D-G was made by spin-coating the metal chlorides on P-G at 3000 rpm for 60 s after a residual time of 60 s. The doping concentration was fixed at 20 mM, as reported previously.[14,15] The transfer of the P-G sheet and doping process were repeated four times for the fabrication of multilayer D-G.

Fabrication of LEDs: The p-type GaN substrates were grown on a c-plane (0001) sapphire using metal-organic chemical vapor deposition. They consisted of a 500 nm thick undoped GaN buffer layer, 4 μm thick n-type GaN, InGaN/GaN multiple quantum well, p-type AlGaN electron blocking layer, and multiple p-type GaN layers. The substrate was cleaned using piranha solution (H_2SO_4/H_2O_2 = 1:1 volume ratio) and by boiling aqua regia (HCl/HNO_3 = 1:3 volume ratio) for 10 min to remove the oxide residue on the surface. Two kinds of LED fabrication process are compared, as shown in Fig. 1. The difference is the process sequence of D-G transfer and ICP etching. In *PROCESS I*, P-G was directly transferred to and doped on the GaN substrate. After D-G fabrication, mesa etching was carried out using ICP with a photoresist (PR) to open the n-type GaN layer. The graphene-transferred p-type GaN was dry etched using 3 min of ICP etching to open the n-type GaN using a mixture of Cl_2 (7 sccm) and BCl_3 (3 sccm) gas at a working pressure of 5 mTorr, a plasma power of 350 W, and a chuck bias of 100 W.[16] Then, the p-pad and n-pad, consisting of Cr/Au (50 nm / 300 nm), were deposited onto the substrate. The chip size of LED is 300 × 300 μm^2.

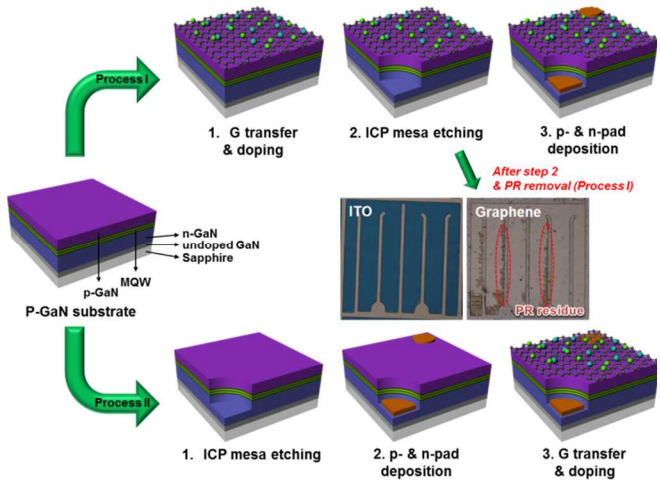

FIG. 1. Schematic illustration of the GaN light-emitting diode (LED) fabrication processes. *PROCESS I* and *PROCESS II* are compared in this experiment.

As shown in the inset of Fig. 1, the amount of remaining PR residue on graphene was considerable after ICP mesa etching, which was not shown on the ITO electrode. It seems that PR easily reacted with graphene due to the addition of energy from ICP because PR and graphene are composed of carbon atoms. The PR residue could be an obstacle to uniform current spread in LEDs. Furthermore, it is reported that the graphene was severely damaged and split into submirometer-scale islands by the high-energy ICP etching process.[17] In *PROCESS II*, ICP mesa etching was performed before D-G transfer. D-G was transferred to the etched p-type GaN substrate with the p-pad and n-pad. The D-G was patterned by using O_2 plasma. No PR residue was found on the D-G layer surface, so the current is expected to spread uniformly.

Characterization: The sheet resistance was measured in a standard state using a four-point probe technique (Keithley 2612A multimeter, U.S.A.). UV-visible spectra were recorded using a JASCO V-740 photo-spectrometer with a wavelength range of 400–900 nm. FE-SEM (JEOL, JSM-5410LV, Japan) images of the P-G and D-G films were also obtained. The graphene Raman spectra were obtained using a Lab RAM HR (Horiba JobinYvon, Japan) at an excitation wavelength of 514.54 nm. Synchrotron radiation photoelectron spectroscopy (SRPES) experiments were performed in an ultra-high vacuum chamber (base pressure of approximately 10^{-10} Torr) in a 4D beam line, equipped with an electron analyser and a heating element, at the Pohang Acceleration Laboratory. The onset of photoemission, corresponding to the vacuum level at the graphene surface, was measured using an incident photon energy of 250 eV with a negative bias on the sample. The results were corrected for charging effects by using Au 4*f* as an internal reference.

Results and Discussion

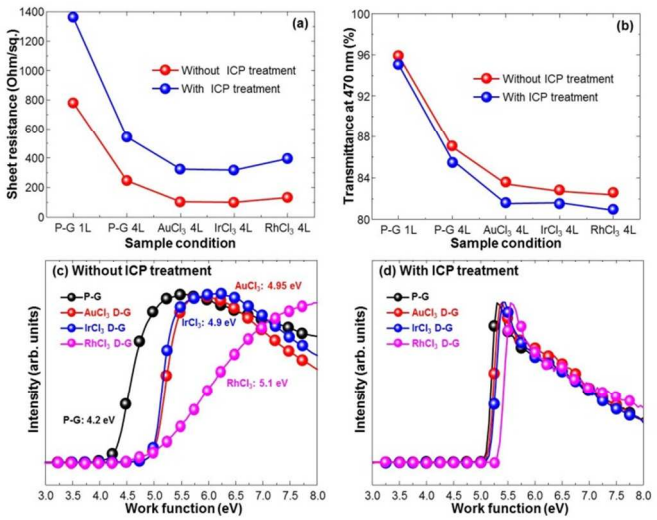

Fig. 2. (a) Sheet resistances of single layer pristine graphene (P-G 1L), P-G 4L, $AuCl_3$ doped graphene (D-G) 4L, $IrCl_3$ D-G 4L, and $RhCl_3$ D-G 4L before and after inductively coupled plasma (ICP) etching. (b) The transmittance values at 550 nm for P-G 1L, P-G 4L, $AuCl_3$ D-G 4L, $IrCl_3$ D-G 4L, and $RhCl_3$ D-G 4L samples before and after ICP etching.

To investigate the effect of ICP etching on the electrical and optical properties of P-G and D-G, the values of sheet resistance and transmittance at 470 nm were measured using a four-point probe method and UV-visible spectroscopy, as shown in Fig. 2(a) and (b). The samples were coated with PR and then the ICP treatment was performed under the same conditions used during LED fabrication. After ICP treatment, the PR was removed by using a 3:1 ratio of an acetone:chloroform boiling solution. Before ICP treatment, the sheet resistance decreased from 780 Ω/sq for P-G to 220, 110, 105, and 140 Ω/sq for 4-layer (4L) G, $AuCl_3$, $IrCl_3$, and $RhCl_3$ D-G,

respectively. However, after treatment, the sheet resistance considerably increased to 1350, 540, 320, 315, and 395 Ω/sq for P-G, P-G 4L, $AuCl_3$, $IrCl_3$, and $RhCl_3$ D-G, respectively, indicating that ICP treatment degrades the electrical properties of graphene.

The transmittance at 470 nm of each sample decreased from 87% to 83–84% after doping. After ICP treatment, the values of transmittance more decreased to 95, 85, 81.5, 81.5, and 80.5% for P-G 1L, P-G 4L, $AuCl_3$, $IrCl_3$, and $RhCl_3$ D-G, respectively. As shown in the inset of Fig. 1, the PR layer reacted strongly with the graphene layers when the harsh ICP etching was performed, causing PR residue to remain on the surface of graphene. PR residue on graphene films is thought to induce the increase in sheet resistance and the decrease in transmittance after the ICP etching process.

Secondary electron cutoff spectra of graphene with and without ICP treatment were shown in Fig. 2(c) and (d) to identify the value of the work function. The value of the work function was calculated using the following equation:

$$\Phi = h\nu - E_{th} \quad (1)$$

Here, Φ is the value of the work function, hν is the photon energy of the excitation light (He I discharge lamp, 21.2 eV), and E_{th} is electron threshold energy. The secondary electron threshold energy was determined by extrapolating two solid lines from the background and straight onset in the secondary electron cutoff spectra.[18,19] The value of the work function, Φ, of D-G increased from 4.2 eV for P-G to 4.95, 4.9, and 5.1 eV for $AuCl_3$, $IrCl_3$, and $RhCl_3$ D-G, respectively. After ICP treatment, Φ of P-G increased from 4.2 eV to 5.0 eV. It is thought that the combination of graphene and PR induces a hole trapping phenomena based on the electron tail reduction model, resulting in the increase of Φ.[20,21] However, Φ of other D-G samples did not increase after ICP etching in comparison to P-G cases. It is considered that the hole trapping phenomena induced by the PR is marginal due to the chlorine anion in D-G samples.

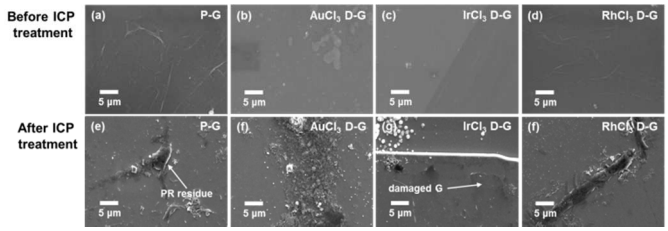

Fig. 3. The field-emission scanning electron microscopy (FE-SEM) images of P-G and each different D-G sample before and after the ICP etching process. (a) P-G, (b) $AuCl_3$, (c) $IrCl_3$, and (d) $RhCl_3$ D-G before ICP etching. (e) P-G, (f) $AuCl_3$, (g) $IrCl_3$, and (h) $RhCl_3$ D-G after ICP etching.

Fig. 3 shows the FE-SEM images of the samples before and after ICP etching. Some particles are observed on D-G samples that are not shown on the P-G sample. These particles are thought to be metal nanoparticles induced by spontaneous charge transfer from graphene to metal chlorides. Therefore, these metal nanoparticles decreased the transmittance values of D-G as shown in Fig. 2(b).

After the ICP etching process, PR residue and damaged graphene sheets were observed on the graphene surface in all the samples. This residue led to increased and decreased values of sheet resistance and transmittance of P-G and D-G. Furthermore, the size of the metal particles became larger and brighter after ICP treatment, indicating that the treatment induced metal particle agglomeration. These data indicated that the ICP process damaged graphene, degrading its properties.[22,23]

Fig. 4(a) and (b) show the Raman spectra of P-G and D-G samples before and after the ICP etching process. The G peaks are located at 1583, 1588, 1590, and 1588 cm^{-1} for P-G, $AuCl_3$, $IrCl_3$, and $RhCl_3$ D-G, respectively. The locations of G peaks in D-G were higher wavenumbers compared to the G peak in P-G. Furthermore, 2D peaks of D-G samples were shown to be shifted to higher wavenumbers compared to the 2D peak of P-G. These results agree with previous articles, which reported that both hole and electron doping on graphene made G and 2D peaks shift to higher wavenumbers.[24,25] Therefore, it is thought that the graphene sheet was effectively doped with metal chloride solution. After ICP treatment was performed on graphene, the position of G and 2D peak in D-G samples were downshifted to lower wavenumber. The G and 2D peak positions were plotted before and after ICP etching to clarify this issue, as shown in Fig. 4(c). Furthermore, the intensity of the D peak significantly increased after ICP treatment. The intensity ratios of the D peak to the G peak increased after the ICP etching process, as shown in Fig. 4(d). Therefore, it is thought that the graphene sheets were damaged by ICP etching and reacted with PR residue.

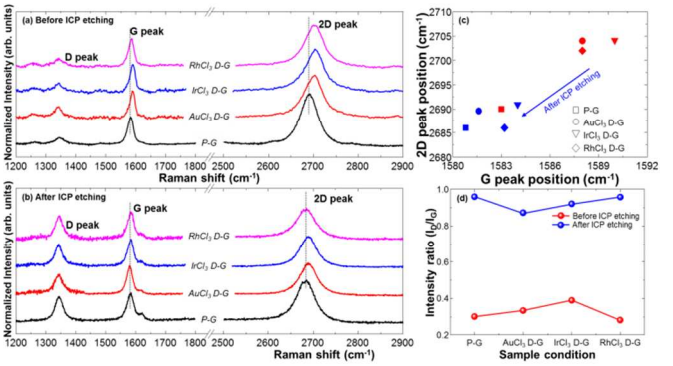

Fig. 4. (a) The Raman spectra of the metal chloride D-G before ICP etching. The positions of the G and 2D peaks in D-G were shifted to higher wavenumbers compared to those of P-G. (b) The Raman spectra of metal chloride D-G after ICP etching. The intensity of the D peak increased and the G and 2D peak positions of D-G matched those of P-G after ICP etching. (c) The intensity ratio of the D peak to the G peak before and after ICP etching. The inset graph shows the intensity ratio of the 2D peak to the G peak. (d) The G and 2D peak positions of P-G and D-G samples before and after ICP etching. Red color indicates the states before ICP etching and blue color indicates the states after ICP etching.

The current-voltage (I-V) characteristics of the GaN-based LEDs with P-G and D-G electrodes made using *PROCESS II* are displayed in Fig. 5(a). The number of graphene layers was fixed at four. The device forward voltage (V_F) at a 10 mA current was 5.9 V for P-G electrode. This V_F value is higher than ITO-based LEDs, which was recently reported to be 4 V.[7] The V_F of LEDs with D-G electrodes at an injection current of 10 mA was lowered from 5.9 V to 4.4, 4.25, and 4.5 V for $AuCl_3$, $IrCl_3$, and $RhCl_3$ D-G, respectively. It is thought that the decreased sheet resistance and increased Φ in D-G enhanced the electrical properties of LEDs.[8,12] The V_F at a 10 mA injection current was 5.5 V for LEDs with P-G and D-G electrodes in *PROCESS I*. It is reported that thermal degradation occurred in D-G, leading to Φ of D-G returning to the value of Φ of P-G and

increased sheet resistance.[9] The ICP etching process thermally heated the graphene, meaning the I-V difference between P-G and D-G LEDs was not found in *PROCESS I*. The current injected optical images of LEDs fabricated using *PROCESS II* are displayed in Fig. 5(b). LEDs with P-G electrodes exhibited strong current crowding around the p-pad. However, the light emission properties of LEDs with D-G electrodes were shown to be significantly enhanced in *PROCESS II*. The LED with an $IrCl_3$ D-G electrode displayed the best light emission properties at a 5 mA current. Neither P-G nor D-G exhibited PR residue in *PROCESS II*, and the emission difference between the P-G D-G electrodes was magnified as a result. In the case of LEDs made using *PROCESS I*, the PR residue interrupts the current spreading properties of the graphene sheet. Graphene carrier transport properties deteriorated because high temperatures induced by ICP mesa etching promoted the reaction between graphene and PR. Furthermore, the graphene current spreading layer might have been damaged during the ICP etching step because of the harsh ion bombardment treatment on the GaN substrate. These results indicated that the current injection properties of D-G are better that those of P-G.

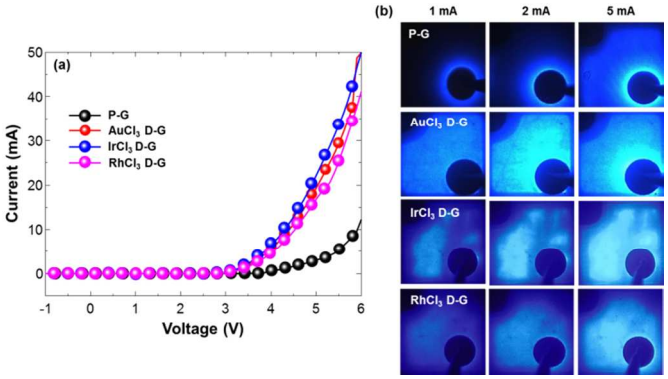

Fig. 5. (a) Device current-voltage (I-V) characteristics of LEDs with four different electrodes from *PROCESS II*. The P-G, $AuCl_3$, $IrCl_3$, and $RhCl_3$ D-G were used as electrodes. (b) The light emission images of LEDs fabricated using *PROCESS II*. The image of $IrCl_3$ D-G at an injection current of 5 mA is the brightest among all of the samples.

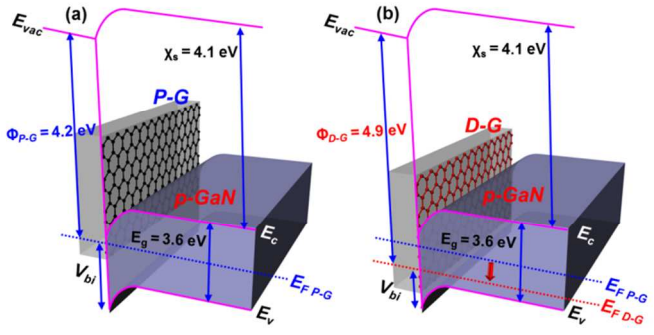

Fig. 6. Schematic energy band diagram in (a) P-G/p-type GaN and (b) D-G/p-type GaN. The hole injection barrier height was lowered by doping with graphene.

Figs. 6(a) and (b) show the band diagrams of P-G/p-type GaN and D-G/p-type GaN. The E_{vac}, ϕ, E_c, E_v, X_s, and V_{bi} mean vacuum energy level, work function, conduction band, valence band, energy gap between vacuum level and conduction band of p-type GaN, and injection barrier height, respectively. The energy levels for p-type GaN were adopted from previous reports.[26-28] The value of Φ of D-G increased from 4.2 eV to 4.9–5.1 eV, as shown in Fig. 2(c). This led to a drop in the Fermi level (E_F in the figure) of graphene. This induced the decrease of V_{bi} in D-G/p-type GaN, improving the hole injection into p-type GaN. Therefore, it is thought that D-G without ICP treatment lowers the injection barrier of p-type GaN, enhancing light emission and I-V characteristics.

Conclusions

Two kinds of LED fabrication processes were investigated using P-G and D-G electrodes. The sheet resistance decreased from 220 Ω/sq to 105–140 Ω/sq, and the value of the work function increased from 4.2 eV to 4.9–5.1 eV for 4L D-G. The graphene electrode was treated using ICP during mesa etching step in *PROCESS I*. In *PROCESS II*, the graphene electrode was transferred after the mesa etching step so that graphene was not treated by ICP. The V_F at an injection current of 10 mA was 5.5 V for LEDs with P-G and D-G electrodes in *PROCESS I*. No difference was found in the I-V and luminance characteristics between P-G and D-G LEDs fabricated through *PROCESS I* because the ICP etching process thermally heated graphene. In the case of LEDs using D-G as electrodes in *PROCESS II*, the V_F at an injection current of 10 mA was lowered to 4.25–4.5 V and luminance properties were improved compared to the LED with the P-G electrode. It is thought that the decreased sheet resistance and increased work function value in D-G enhanced LED electrical properties. These findings provide a potential basis for the application of graphene electrodes in GaN-based LEDs.

Acknowledgements

This research was supported by the Center for Green Airport Pavement Technology (CGAPT) of Chung-Ang University.

Notes and references

[a] School of Chemical Engineering and Materials Science, Chung-Ang University, Seoul 156-756, Korea
[b] Department of Materials Science and Engineering, Pohang University of Science and Technology (POSTECH), Pohang, Gyeongbuk 790-784, Republic of Korea

1 S. Nakamura, T. Mukai, M. Senoh, N. Iwasa, *Jpn. J. Appl. Phys.*, 1992, **31**, L139.
2 S.-P. Jung, D. Ullery, C.-H. Lin, H. P. Lee, J.-H. Lim, D.-K. Hwang, J.-Y. Kim, E.-J. Yang, S.-J. Park, *Appl. Phys. Lett.*, 2005, **87**, 181107.
3 T. Neubert, F. Neumann, K. Schiffmann, P. Willich, A. Hangleiter, *Thin Solid Films*, 2006, **513**, 319-324.
4 A. K. Geim, K. S. Novoselov, *Nat. Mater.*, 2007, **6**, 183-191.
5 J. C. Meyer, A. K. Geim, M. I. Katsnelson, K. S. Novoselov, T. J. Booth, S. Roth, *Nature*, 2007, **446**, 60-63.

6 K. S. Novoselov, A. K. Geim, S. V. Morozov, D. Jiang, M. I. Katsnelson, I. V. Grigorieva, S. V. Dubonos, A. A. Firsov, *Nature*, 2005, **438**, 197-200.
7 Y. Hernandez, V. Nicolosi, M. Lotya, F. M. Blighe, Z. Sun, S. De, I. T. Mcgovern, B. Holland, M. Bryne, Y. K. Gunko, J. J. Boland, P. Niraj, G. Duesberg, S. Krishnamurthy, R. Goodhue, J. Hutchison, V. Scardaci, A. C. Ferrari, J. N. Coleman, *Nat. nanotechnol.*, 2008, **3**, 563-568.
8 J. M. Lee, H. Y. Jeong, K. J. Choi, W. I. Park, *Appl. Phys. Lett.*, 2011, **99**, 041115.
9 S. Chandarmohan, J. H. Kang, Y. S. Katharria, N. Han, Y. S. Beak, K. B. Ko, J. B. Park, H. K. Kim, E.-K. Suh C.-H. Hong, *Appl. Phys. Lett.*, 2012, **100**, 023502.
10 W.-C. Lai, C.-N. Lin, Y.-C. Lai, P. Yu, G. C. Chi, S.-J. Chang, *Optics express*, 2014, **22**, A396.
11 K. Xu, C. Xu, Y. Xie, J. Deng, Y. Zhu, W. Guo, M. Mao, M. Xun, M. Chen, L. Zheng, J. Sun, *Appl. Phys. Lett.*, 2013, **103**, 222105.
12 G. Jo, M. Choe, C.-Y. Cho, J. H. Kim, W. Park, S. Lee, W.-K. Hong, T.-W. Kim, S.-J. Park, B. H. Hong, Y. H. Kahng, T. Lee, *Nanotechnology*, 2010, **21**, 175201.
13 Y. S. Kim, K. Joo, S.-K. Jerng, J. H. Lee, D. Moon, J. Kim, E. Yoon, S.-H. Chun, *ACS nano*, 2014, **8**, 2230-2236.
14 K. C. Kwon, K. S. Choi, S. Y. Kim, *Adv. Funct. Mater.*, 2012, **22**, 4724-4731.
15 K. C. Kwon, B. J. Kim, J.-L. Lee, S. Y. Kim, *J. Mater. Chem. C*, 2013, **1**, 253-259.
16 J. H. Son, J. U. Kim, Y. H. Song, B. J. Kim, C. J. Ryu, J.-L. Lee, *Adv. Mater.*, 2012, **24**, 2259-2262.
17 K. Joo, S.-K. Jerng, Y. S. Kim, B. Kim, S. Moon, D. Moon, G.-D. Lee, Y.-K. Song, S.-H. Chun, E. Yoon, *Nanotechnology*, 2012, **23,** 425302.
18 K. C. Kwon, K. S. Choi, C. Kim, S. Y. Kim, *J. Phys. Chem. C*, 2014, **118**, 8187-8193.
19 K. C. Kwon, K. S. Choi, C. Kim, S. Y. Kim, *Phys. Status Solidi A-applications and materials science*, 2014, DOI 10.1002/pssa.201330444.
20 S. Y. Kim, K. Hong, J.-L. Lee, *Appl. Phys. Lett.*, 2007, **90**, 183508.
21 K. C. Kwon, S. Y. Kim, *Chem, Eng. J.*, 2014, **244**, 355-363..
22 S. M. Kim, K. K. Kim, Y. W. Jo, M. H. Park, S. J. Chae, D. L. Duong, C. W. Yang, J. Kong, Y. H. Lee, *ACS nano*, 2011, **5**, 1236-1242.
23 K. C. Kwon, P. K. Son, S. Y. Kim, *Carbon*, 2014, **67**, 352-359.
24 A. Das, S. Pisana, B. Chakraborty, S. Piscanec, S. K. Saha, U. V. Waghmare, K. S. Novoselov, H. R. Krishnamurthy, A. K. Geim, A. C. Ferrari, A. K. Sood, *Nat. Nanotechnol.*, 2008, **3**, 210-215.
25 Q. H. Wang, Z. Jin, K. K. Kim, A. J. Hilmer, G. L. C. Paulus, C.-J. Shih, M.-H. Ham, J. D. Sanchez-Yamagishi, K. Watanabe, T. Taniguchi, J. Kong, P. Jarillo-Herrero, M. S. Strano, *Nat. Chem.*, 2012, **4**, 724-732.
26 M. E. Lin, F. Y. Huang, Z. F. Fan, L. H. Allen, H. Morkoc, *Appl. Phys. Lett.*, 1994, **64**, 1003-1005.
27 N. Sarkar, S. Ghosh, *Solid State Comm.*, 2009, **149**, 1288-1291.
28 J. Piprek, S. Li, Optoelectronic devices: advanced simulation and analysis, 2005, vol. 1, ch. 10, pp. 293-312.

The table of contens entry

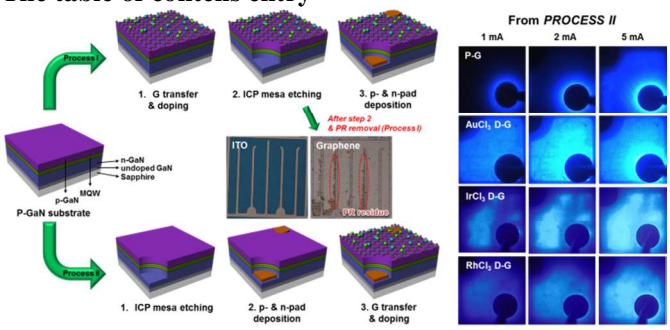

The decrease in the sheet resistance and increase in the value of the work function in doped graphene (D-G) enhanced the electrical properties of the light emitting diodes (LEDs). Therefore, avoiding the inductively coupled plasma etching step is better for D-G electrodes in GaN-based LEDs.

Keywords: light-emitting diodes, graphene, doping, work-function, polymer residue

Author: Ki Chang Kwon,[a] Buem Jun Kim,[b] Cheolmin Kim,[a] Jong-Lam Lee,[*b] and Soo Young Kim[*a]

Title: Comparison of metal chloride-doped graphene electrode fabrication proecess for GaN-based light emitting diodes